0026-895X/11/8003-426–433$25.00
MOLECULAR PHARMACOLOGY

Mol Pharmacol 80:426–433, 2011

Vol. 80, No. 3
72504/3711592
Printed in U.S.A.

Batrachotoxin, Pyrethroids, and BTG 502 Share Overlapping Binding Sites on Insect Sodium Channels[S]

Yuzhe Du, Daniel Garden, Bhupinder Khambay, Boris S. Zhorov, and Ke Dong

Department of Entomology, Genetics and Neuroscience Programs, Michigan State University, East Lansing, Michigan (Y.D., K.D.); Department of Biochemistry and Biomedical Sciences, McMaster University, Hamilton, Ontario, Canada (D.G., B.S.Z.); Biological Chemistry Division, Rothamsted Research Ltd, Harpenden, Hertfordshire, United Kingdom (B.K.); and Sechenov Institute of Evolutionary Physiology and Biochemistry, Russian Academy of Science, St. Petersburg, Russia (B.S.Z.)

Received March 30, 2011; accepted June 3, 2011

ABSTRACT

Batrachotoxin (BTX), a steroidal alkaloid, and pyrethroid insecticides bind to distinct but allosterically coupled receptor sites on voltage-gated sodium channels and cause persistent channel activation. BTX presumably binds in the inner pore, whereas pyrethroids are predicted to bind at the lipid-exposed cavity formed by the short intracellular linker-helix IIS4-S5 and transmembrane helices IIS5 and IIIS6. The alkylamide insecticide (2*E*,4*E*)-*N*-(1,2-dimethylpropyl)-6-(5-bromo-2-naphthalenyl)-2,4-hexadienamide (BTG 502) reduces sodium currents and antagonizes the action of BTX on cockroach sodium channels, suggesting that it also binds inside the pore. However, a pyrethroid-sensing residue, Phe^{3i17} in IIIS6, which does not face the pore, is essential for the activity of BTG 502 but not for BTX. In this study, we found that three additional deltamethrin-sensing residues in IIIS6, Ile^{3i12}, Gly^{3i14}, and Phe^{3i16} (the latter two are also BTX-sensing), and three BTX-sensing residues, Ser^{3i15} and Leu^{3i19} in IIIS6 and Phe^{4i15} in IVS6, are all critical for BTG 502 action on cockroach sodium channels. Using these data as constraints, we constructed a BTG 502 binding model in which BTG 502 wraps around IIIS6, probably making direct contacts with all of the above residues on the opposite faces of the IIIS6 helix, except for the putative gating hinge Gly^{3i14}. BTG 502 and its inactive analog DAP 1855 antagonize the action of deltamethrin. The antagonism was eliminated by mutations of Ser^{3i15}, Phe^{3i17}, Leu^{3i19}, and Phe^{4i15} but not by mutations of Ile^{3i12}, Gly^{3i14}, and Phe^{3i16}. Our analysis revealed a unique mode of action of BTG 502, its receptor site overlapping with those of both BTX and deltamethrin.

Introduction

Voltage-gated sodium channels (Na_V) are responsible for the rapid rising phase of action potentials in electrically excitable cells. The pore-forming subunits of Na_V channels contain four homologous repeats, each having six transmembrane helices (S1–S6). Helices S1 to S4 form the voltage-sensing domain and transmembrane helices S5 (outer helix) and S6 (inner helix) contribute to the pore-forming domain. The residues connecting the S5 and S6 transmembrane helices form the four re-entrant loops, called P-loops. These P-loops contain the amino acid residues that confer the ion selectivity in Na_V. The voltage sensor is linked to the outer helix S5 by a short intracellular linker helix S4–S5.

Na_V are targets of diverse natural and synthetic toxins, including therapeutic drugs, insecticides (such as pyrethroids), and naturally occurring toxins [such as batrachotoxin (BTX)]. Toxins from each group bind to distinct receptor sites on sodium channels and affect channel function (Wang and Wang, 2003). BTX (Fig. 1), isolated from the skin of a Colombian frog (Daly et al., 1965), reduces ion selectivity and causes persistent channel activation by inhibiting inactivation and shifting the voltage dependence of activation in the hyperpolarizing direction. Pyrethroids, such as deltamethrin (Fig. 1), are synthetic derivatives of the naturally occurring pyrethrum insecticides extracted from *Chrysanthemum* species (Elliott, 1977). Pyrethroids bind to a unique receptor site and inhibit deactivation and inactivation, resulting in prolonged opening of sodium channels (Vijverberg and van den Bercken, 1990; Bloomquist, 1996; Narahashi, 2000).

BTX was believed to bind at the lipid-channel interface and alter channel selectivity and gating by an allosteric mecha-

This study was supported by the National Institutes of Health National Institute of General Medical Sciences [Grant GM057440] and the Natural Sciences and Engineering Research Council of Canada [Grant GRPIN/238773-2009]. Computations were performed using the facilities of the Shared Hierarchical Academic Research Computing Network (http://www.sharcnet.ca).

Y.D. and D.G. contributed equally to this work.

Article, publication date, and citation information can be found at http://molpharm.aspetjournals.org.
doi:10.1124/mol.111.072504.

[S] The online version of this article (available at http://molpharm.aspetjournals.org) contains supplemental material.

ABBREVIATIONS: Na_V, Voltage-gated sodium channel; BTX, batrachotoxin; BTG 502, (2*E*,4*E*)-*N*-(1,2-dimethylpropyl)-6-(5-bromo-2-naphthalenyl)-2,4-hexadienamide; DMSO, dimethyl sulfoxide; MC, Monte Carlo; $BgNa_V$, cockroach sodium channel.

nism (Linford et al., 1998). However, mutational studies identified BTX-sensing residues in the inner helices of all four domains, suggesting that BTX is directly exposed to the permeation pathway (Tikhonov and Zhorov, 2005b). More recent mutational and modeling studies have confirmed this prediction (Wang et al., 2006, 2007a,b; Du et al., 2011a). Studies of the mechanisms of insect resistance to pyrethroids led to the identification of pyrethroid-sensing residues in diverse regions of insect sodium channels (Soderlund, 2005; Davies et al., 2007; Dong, 2007). These data have been used to construct a model of the sodium channel in which pyrethroids bind to a cavity formed by the linker-helix IIS4–S5, the outer helix IIS5, and the inner helix IIIS6 at the interface between domains II and III (O'Reilly et al., 2006). Systematic site-directed mutagenesis of residues in IIIS6 revealed additional four residues that are important for the action of deltamethrin (Du et al., 2009), and two of them are also critical for the action of BTX (Du et al., 2011a). Despite this apparent overlap, the binding sites for BTX and pyrethroids in IIIS6 are distinct, involving opposite faces of the IIIS6 transmembrane helix (Du et al., 2009).

An alkylamide insecticide, (2*E*,4*E*)-*N*-(1,2-dimethylpropyl)-6-(5-bromo-2-naphthalenyl)-2,4-hexadienamide (BTG 502; Fig. 1), has been shown to antagonize the binding and action of BTX in ligand-binding and $^{22}Na^{+}$ influx assays using mouse brain synaptoneurosomes (Ottea et al., 1989, 1990). These results suggest that BTG 502 and BTX compete for a common receptor site on sodium channels (Ottea et al., 1989). However, recent data indicate that BTG 502, unlike BTX, acts as an antagonist, reducing the peak current of insect sodium channels expressed in *Xenopus laevis* oocytes (Du et al., 2011b). In addition, Phe^{3i17} in IIIS6,[1] a residue important for pyrethroid activity, is also critical for the action of BTG 502 (Du et al., 2011b) but not for that of BTX (Tan et al., 2005). These results suggest that BTG 502 and BTX must have somewhat distinct binding and/or action properties that translate into distinct electrophysiological effects.

Here we conducted mutational analysis and molecular modeling to map the binding site of BTG 502. We found that three additional deltamethrin-sensing residues (two of which are also BTX-sensing) and three BTX-sensing residues are critical for BTG 502 action. Our model incorporates available experimental data on the action of BTG 502 on the cockroach sodium channel $BgNa_v$ and suggests that BTG 502 makes contact with residues on opposite faces of the IIIS6 helix. Therefore, the receptor site for BTG 502 on sodium channels is a unique receptor site that overlaps those of BTX and pyrethroids.

Materials and Methods

Expression of $BgNa_v$ Sodium Channels in *X. laevis* Oocytes. The procedures for oocyte preparation and cRNA injection are identical to those described previously (Tan et al., 2002). For robust expression of the $BgNa_v$ sodium channels, cRNA was coinjected into oocytes with *Drosophila melanogaster* tipE cRNA (1:1 ratio), which enhances the expression of insect sodium channels in oocytes (Feng et al., 1995; Warmke et al., 1997).

Electrophysiological Recording and Data Analysis. Sodium currents were recorded using standard two-electrode voltage clamping. The borosilicate glass electrodes were filled with filtered 3 M KCl in 0.5% agarose and had a resistance of 0.5 to 1.0 MΩ. The recording solution was ND-96, consisting of 96 mM NaCl, 2.0 mM KCl, 1.0 mM $MgCl_2$, 1.8 mM $CaCl_2$, and 10 mM HEPES, pH adjusted to 7.5 with NaOH. Sodium currents were measured with an oocyte clamp (OC-725C; Warner Instruments, Hamden, CT) and processed with a Digidata 1322A interface (Molecular Devices, Sunnyvale, CA). Data were sampled at 50 kHz and filtered at 2 kHz. Leak currents were corrected by p/4 (pulse/number) subtraction. pClamp 9.2 software (Molecular Devices) was used for data acquisition and analysis. The maximal peak sodium current was limited to <2.0 μA to achieve optimal voltage control by adjusting the amount of cRNA injected and the incubation time after injection.

To measure the effect of BTG 502 on the sodium channel, sodium currents were elicited by a 20-ms test pulse to −10 mV from a holding potential of −120 mV after 100 repetitive depolarizing pulses to −10 mV at 10 Hz (Du et al., 2011b). The pyrethroid-induced tail current was recorded during a 100-pulse train of 5-ms depolarization from −120 to 0 mV with a 5-ms interpulse interval. The percentage of channels modified by pyrethroids was calculated using the equation $M = \{[I_{tail}/(E_h - E_{Na})]/[I_{Na}/(E_t - E_{Na})]\} \times 100$ (Tatebayashi and Narahashi, 1994), where I_{tail} is the maximal tail current amplitude, E_h is the potential to which the membrane is repolarized, E_{Na} is the reversal potential for sodium current determined from the current-voltage curve, I_{Na} is the amplitude of the peak current during depolarization before pyrethroid exposure, and E_t is the potential of step depolarization.

Data analyses were performed using pClamp 9.2 (Molecular Devices), Origin 8.1(OriginLab Corp, Northampton, MA), and Adobe Illustrator (Adobe Systems, San Jose, CA) software. Results are

[1] We use a residue-labeling scheme that is universal for P-loop channels. A residue label includes the domain (repeat) number (1–4), segment type (p, P-loop; i, inner helix; o, outer helix), and relative position of the residue in the segment (Table 1).

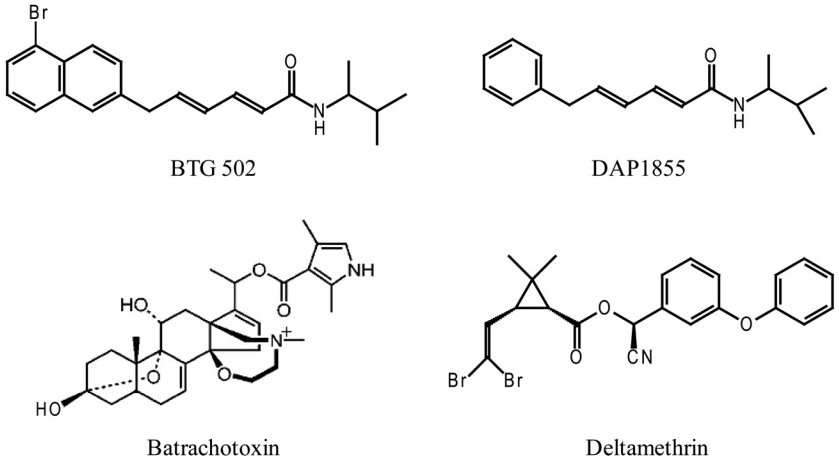

Fig. 1. Chemical structures of BTG 502, DAP 1855, batrachotoxin, and deltamethrin.

reported as mean ± S.D. Statistical significance was determined by using one-way analysis of variance with Scheffé's post hoc analysis, and significant values were set at $p < 0.05$ as indicated in the figure legend.

Chemicals. BTG 502 and an inactive analog, DAP 1855 (Fig. 1), were provided by Rothamsted Research Ltd. (Harpenden, UK). BTX and deltamethrin were generous gifts from John Daly (National Institutes of Health, Bethesda, MD) and Klaus Naumann and Ralf Nauen (Bayer CropScience AG, Monheim, Germany), respectively. Stock solutions of BTX (1 mM), BTG 502 (50 mM), and deltamethrin (100 mM) were made in dimethyl sulfoxide (DMSO). The working concentration was prepared in ND96 recording solution immediately before the experiments. The concentration of DMSO in the final solution was <0.5%, which had no effect on the function of sodium channels in the experiments. The method for application of chemicals in the recording system was identical to that described previously (Tan et al., 2002) Effects of deltamethrin, BTX, and BTG 502 were measured 10 min after toxin application.

Homology Model of $BgNa_v1.1$. A homology model of the open cockroach sodium channel variant $BgNa_v1$-1 was constructed based on the crystal structure of $K_v1.2$-$K_v2.1$ chimera channel (Long et al., 2007). Amino acid sequences of the pore domains of $BgNa_v1$-1 (Fig. 2A) and $K_v1.2$ were aligned as before (Zhorov and Tikhonov, 2004; Bruhova et al., 2008), and positions of residues are labeled using a universal scheme (Zhorov and Tikhonov, 2004) (see Table 1). The extracellular loops, which are too far from residues important for BTX and deltamethrin activity, were not included in the model. The P-loops were modeled as in Tikhonov and Zhorov (2005a). Energy was calculated using the AMBER force field (Weiner et al., 1984, 1986) and the solvent exposure- and distance-dependent dielectric function (Garden and Zhorov, 2010). The atomic charges of the toxin molecules were calculated using the Austin model 1 method (Dewar et al., 1985) through MOPAC. Bond angles were varied in the toxins but not in the protein. Energy was minimized in the space of generalized coordinates (Zhorov, 1981, 1983). The Monte Carlo (MC) energy minimization method (Li and Scheraga, 1987) was used to optimize the channel homology model and to dock the ligands. The SCWRL3 program (Canutescu et al., 2003) was used to assign starting conformations of the channel side chains. The ZMM program (http://www.zmmsoft.com) was used to perform all calculations.

Docking BTG 502. Various binding modes of BTG 502 were explored using distance constraints implied by our experimental data (Supplemental Table S1). A constraint is a flat-bottomed parabolic penalty function added to the energy expression. When the distance between a given toxin atom and a given atom in the toxin-sensing residue exceeds the upper limit of the constraint (5 Å in this study), the penalty contribution to the total energy increases sharply, with a force constant of 100 kcal · mol^{-1} · $Å^{-1}$. The flat-bottomed constraint ensures proximity between two atoms but does not impose specific disposition or orientation of chemical groups the atoms belong to (for instance, an H-bond or π-stacking).

To search for the lowest-energy binding modes of BTG 502, we employed our three-stage flexible docking protocol (Garden and Zhorov, 2010). In the first stage, a library of toxin conformers was generated by randomly sampling the toxins' torsion angles, followed by energy minimizations to ensure that all the rings were closed. Ten thousand toxin conformations were generated, and the 10 lowest-energy conformations were collected for docking. In the second stage, the position and orientation of each toxin conformer in the library was sampled 2×10^5 times by assigning random values to six rigid-body degrees of freedom of the toxin. The energy of the toxin-receptor complexes (including the distance-constraint penalties) was calculated without energy minimization, and the 10 lowest energy complexes were collected. In the third stage, the ten collected complexes were refined by a 10^3-step MC minimization and the lowest energy structure was used as the toxin-binding model consistent

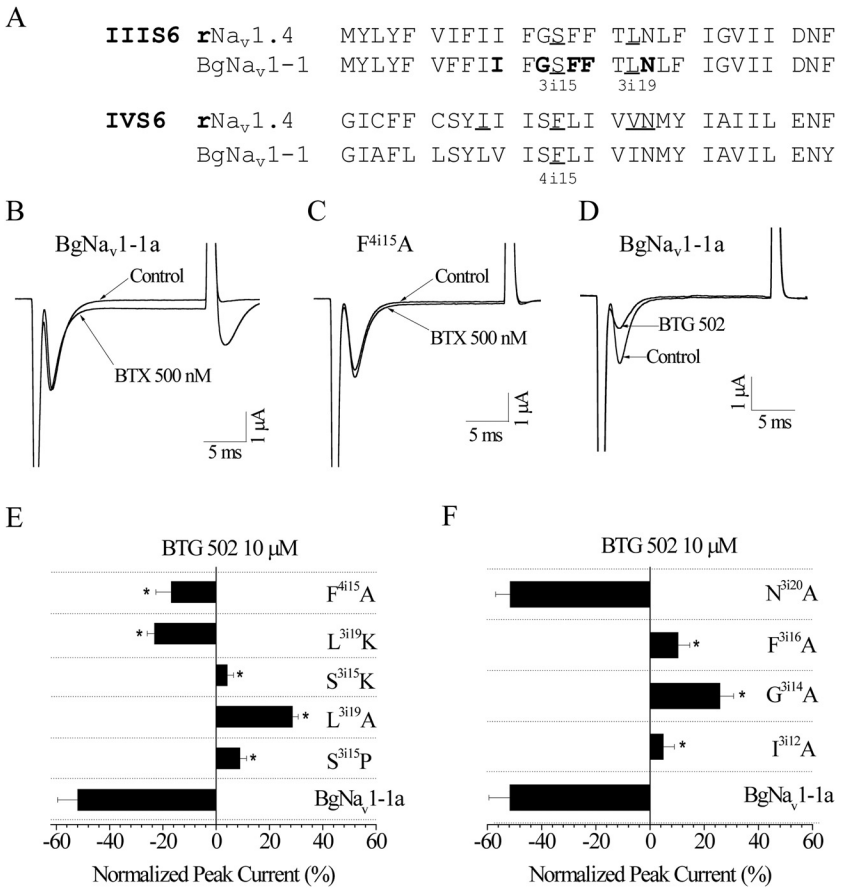

Fig. 2. Both BTX- and pyrethroid-sensing residues are critical for the action of BTG 502. A, amino acid sequences of segments IIIS6 and IVS6 in $rNa_v1.4$ and $BgNa_v$ proteins. BTX-sensing residues Ser^{3i15}, Leu^{3i19}, and Phe^{4i15} are underlined. Pyrethroid-sensing residues Ile^{3i12}, Gly^{3i14}, Phe^{3i16}, Phe^{3i17}, and Asn^{3i20} are in bold. B, effects of BTX (500 nM) on $BgNa_v1$-1a channels. C, substitution $F^{4i15}A$ reduced the action of BTX on $BgNa_v1$-1a channels. D, effects of BTG 502 (10 μM) on $BgNa_v1$-1a channels. E, effects of amino acid substitutions for BTX-sensing residues on peak current inhibition by BTG 502. F, effects of substitutions of pyrethroid-sensing residues on the peak current inhibition by BTG 502 at 10 μM. The peak current reduction by BTG 502 was measured by a 20-ms test pulse to −10 mV from a holding potential of −120 mV after 100 repetitive prepulses to −10 mV at a frequency of 10 Hz before and after the application of 10 μM BTG 502. The asterisks indicate significant differences from the $BgNa_v1$-1a channel as determined by analysis of variance ($p < 0.05$).

with the given combination of distance constraints. At this stage, the torsion angles in the protein side chains and in the toxin were sampled. Finally, all the distance constraints were removed, and the model was MC minimized to check its intrinsic stability. If during the final MC minimization the toxin drifted from the constraints-imposed binding mode, the latter was excluded from further analysis.

Results

Five BTX-Sensing Residues Are Critical for the Action of BTG 502. We have shown previously that lysine substitutions of two amino acid residues in IIIS6, Ser^{3i15} and Leu^{3i19} (Fig. 2A; Supplemental Table S2), dramatically reduce the action of BTX on $BgNa_v1$-1a channels (Du et al., 2009). Residue Phe^{4i15} in IVS6 (Fig. 2A; Supplemental Table S2) is important for the binding and action of BTX on mammalian sodium channels (Linford et al., 1998). Here we show that Phe^{4i15} is also a BTX-sensing residue for $BgNa_v1$-1a channels. BTX (500 nM) inhibited channel inactivation, resulting in a noninactivating current and a tail current associated with repolarization of $BgNa_v1$-1a channels (Fig. 2B). The $F^{4i15}A$ substitution, which was available from another study (Silver et al., 2009), significantly reduced the action of BTX on $BgNa_v1$-1a channels (Fig. 2C).

As reported previously (Du et al., 2011b), the effect of BTG 502 on $BgNa_v1$-1a channels was quite different from those of BTX. In response to 100 repetitive prepulses at a frequency of 10 Hz, BTG 502 reduced the amplitude of peak current of the $BgNa_v1$-1a channel, and no tail current was detected upon repolarization (Fig. 2D). To determine whether Ser^{3i15}, Leu^{3i19} and Phe^{4i15} are also critical for the action of BTG 502, we examined the effect of BTG 502 on the $S^{3i15}P$, $S^{3i15}K$, $L^{3i19}A$, and $L^{3i19}K$ mutant channels that were previously made from $BgNa_v1$-1a channels, as well as the $F^{4i15}A$ mutant channel. While BTG 502 (10 μM) inhibited 50% of the peak current of the $BgNa_v1$-1a channel, it inhibited only 23 and 17% for $L^{3i19}K$ and $F^{4i15}A$ mutant channels, respectively (Fig. 2E). We were surprised to find that BTG 502 increased the amplitude of peak current of the $S^{3i15}P$ and $S^{3i15}K$ channels by 5 to 10% and that of the $L^{3i19}A$ channel by 30% (Fig. 2E).

Four Pyrethroid-Sensing Residues Are Critical for the Action of BTG 502. Our laboratory recently identified four additional residues in IIIS6 (Ile^{3i12}, Gly^{3i14}, Phe^{3i16}, and Asn^{3i20}), besides Phe^{3i17} (Fig. 2A; Supplemental Table S2), that are critical for the action of pyrethroids (Du et al., 2009). In addition, we have shown that Gly^{3i14} and Phe^{3i16} are also critical for the action of BTX (Du et al., 2011a). To determine whether these residues are also critical for the action of BTG 502, we examined the effect of BTG 502 on these four mutant channels. Substitutions $I^{3i12}A$, $G^{3i14}A$, and $F^{3i16}A$ completely abolished the action of BTG 502, whereas substitution $N^{3i20}A$ did not (Fig. 2F; Supplemental Table S2). In fact, BTG 502 increased the amplitudes of peak current of $I^{3i12}A$, $G^{3i14}A$, and $F^{3i16}A$ channels (Fig. 2F).

BTG 502 and Its Inactive Analog DAP 1855 Antagonize the Action of Deltamethrin. To explore possible interactions between BTG 502 and pyrethroids, we examined the response of the $BgNa_v1$-1a channel to deltamethrin in the presence of varying concentrations of BTG 502 or DAP 1855. DAP 1855 is an analog of BTG 502 that has no insecticidal activities but inhibits the binding of BTX to sodium channels in mouse brain synaptoneurosomes (Ottea et al., 1990). With a 100-pulse train of 5-ms step depolarization from −120 to 0 mV at 5-ms intervals, deltamethrin (1 μM) induced a large tail current, as expected for the $BgNa_v1$-1a channel (Fig. 3A). BTG 502 antagonized the effect of deltamethrin by reducing the amplitude of the tail current in a concentration-dependent manner (Fig. 3A). Consistent with the earlier finding (Ottea et al., 1990), DAP 1855 did not affect the peak current of $BgNa_v1$-1a channels (data not shown), but it antagonized the action of deltamethrin (Fig. 3B).

TABLE 1

Sequence alignment

Bold and underlined characters indicate experimentally determined residues that, when mutated, affect action of BTG 502 and deltamethrin, respectively. Position of a residue is designated by a symbol that identifies a segment and a relative position of the residue in the segment.

Channel	Domain	First Residue				
			o1	o11	o21	
KcsA	M1	23	LHWRAAGAAT	VLLVIVLLAG	SYLAVLAER	
$K_v1.2$	S5	323	ASMRELGLLI	FFLFIGVILF	SSAVYFAEA	
$BgNa_v1$-1	IS5	265	ESVKNLRDVI	ILTMFSLSVF	ALMGLQIYM	
	IIS5	902	RTVGALGNLT	FVLCIIIFIF	AVMGMQLFG	
	IIIS5	1397	QAIPSIFNVL	LVCLIFWLIF	AIMGVQLFA	
	IVS5	1715	MSLPALFNIC	LLLFLVMFIF	AIFGMSFFM	
			p33	p41	p51	
KcsA	P	59	LITYPRAL	WWSVETATTV	GYGDLYPV	
$K_v1.2$	P	358	FPSIPDAF	WWAVVSMTTV	GYGDMVPT	
$BgNa_v1$-1	IP	300	CIKNFWAF	LSAFRLMTQD	YWENLYQL	
	IIP	937	VERFPHSF	MIVFRVLCGE	WIESMWDC	
	IIIP	1436	STTLSKAY	LCLFQVATFK	GWIQIMND	
	IVP	1750	GLDDVQSM	ILLFQMSTSA	GWDGVLDG	
			i1	i11	i21	i31
KcsA	M2	86	LWGRLVAVVV	MVAGITSFGL	VTAALATWFV	GREQERR
$K_v1.2$	S6	385	IGGKIVGSLC	AIAGVLTIAL	PVPVIVSNFN	YFYHRET
$BgNa_v1$-1	IS6	402	PWHMLFFIVI	IFLGSFYLVN	LILAIVAMSY	DELQKKA
	IIS6	981	WSCIPFFLAT	VVIGNLVVLN	LFLALLLSNF	GSSNLSA
	IIIS6	1506	IYMYLYFVFF	I**I**F**GSFF**T**L**N	LFIGVIIDNF	NEQKKKA
	IVS6	1806	TVGLAFLLSY	LVIS**F**LIVIN	MYIAVILENY	SQATEDV

o, outer helix; p, P-loop; i, inner helix.

Amino Acid Substitution at Ser^{3i15}, Phe^{3i17}, Leu^{3i19}, and Phe^{4i15} Abolished BTG 502 Antagonism of Deltamethrin Action. Substitutions S^{3i15}P, L^{3i19}A, and F^{4i15}A completely abolished BTG 502 antagonism of deltamethrin action (Fig. 3C; Supplemental Table S2), whereas substitutions I^{3i12}A, G^{3i14}A, F^{3i16}A, and N^{3i20}A did not (Fig. 3D; Supplemental Table S2). At 10 μM, BTG 502 reduced the activity of deltamethrin on BgNa$_v$1-1a channels by 50%. Similar levels of antagonism were observed for substitutions I^{3i12}A, G^{3i14}A, F^{3i16}A, and N^{3i20}A. Because the F^{3i17}I and F^{3i17}A channels are completely insensitive to pyrethroids, and no tail current could be detected (Tan et al., 2005), we used the F^{3i17}W channel, which is approximately 10-fold less resistant to deltamethrin than the F^{3i17}A channel, for this experiment. Unlike other pyrethroid-sensing residues in IIIS6, the F^{3i17}W mutation abolished the BTG 502 antagonism of deltamethrin activity (Fig. 3D).

Docking BTG 502 in the Open Channel. Mutational studies show that BTX binds in the inner pore, contacts the inner helices from all four repeats (Wang et al., 2006, 2007a,b), and may adopt an ion-permeable "horseshoe" conformation within the channel as we recently proposed (Du et al., 2011a). In contrast, pyrethroids including deltamethrin are proposed to bind in the lipid-exposed interface between the linker-helix IIS4–S5, the outer helix IIS5, and the inner helix IIIS6 (O'Reilly et al., 2006; Du et al., 2009). Our data that both BTX- and pyrethroid-sensing residues are critical for the action of BTG 502 indicate that a part of the BTG 502 molecule may bind at the interface between domains II and III, interact with deltamethrin-sensing residues, and interact with residues that face the inner pore.

We used the above data from our mutational and toxin-binding experiments as distance constraints to dock BTG 502 in the channel model. We explored many combinations of distance constraints (Supplemental Table S1) and MC minimized the complex with and then without the distance constraints. The calculations predicted an energetically preferable binding mode, which is most consistent with the experimental data. In this binding mode, BTG 502 wraps around the IIIS6 helix (Fig. 4, A and B). The amide group of the toxin forms a hydrogen bond with Ser^{3i15} (Fig. 4, C and D). The isopropyl group protrudes into the II/III repeat interface, where it interacts with Ile^{3i12} and Phe^{3i16}. The naphthalene ring also protrudes into the III/IV repeat interface where it interacts with Leu^{3i19} and forms π-stacking contacts with Phe^{3i17} and Phe^{4i15} (Fig. 4E). The lipophilic bromine atom faces a hydrophobic site between IIIS6 and IIIS5. The flexible linker of BTG 502 is exposed to the central pore, where it interacts with Leu^{3i19} (Fig. 4, C–E). Thus, BTG 502 makes direct contacts with all the known BTG 502-sensing residues except the gating-hinge Gly^{3i14}. Using this binding mode, we performed further computations to rationalize further experimental observations.

In addition to the BTG 502 binding mode described above, our constraints-driven docking calculations predicted an alternative binding mode in which BTG 502 wraps around IIIS6 from the lipid side (not shown). This binding mode seems unlikely, as described in legend to Supplemental Fig. S1.

Docking BTG 502 in the Closed Channel. The agonistic effect of BTG 502, when applied to sodium channels in combination with scorpion toxin (Ottea et al., 1989), suggests that BTG 502 stabilizes the open conformation of sodium channels. Our data showing that BTG 502 had no effect without a train of depolarizing prepulses (Du et al., 2011b) indicates preferable binding to open channels. To suggest a possible cause of this state-dependent action, we docked BTG 502 into the KcsA-based homology model of closed BgNa$_v$1-1 channels. We imposed toxin-channel distance constraints to mimic in the closed channel the BTG 502 binding mode, which we predicted for the open channel. MC minimizations yielded a high-energy complex in which the inner helices were bent at the site where the aromatic ends of BTG 502 protruded into the domain interfaces

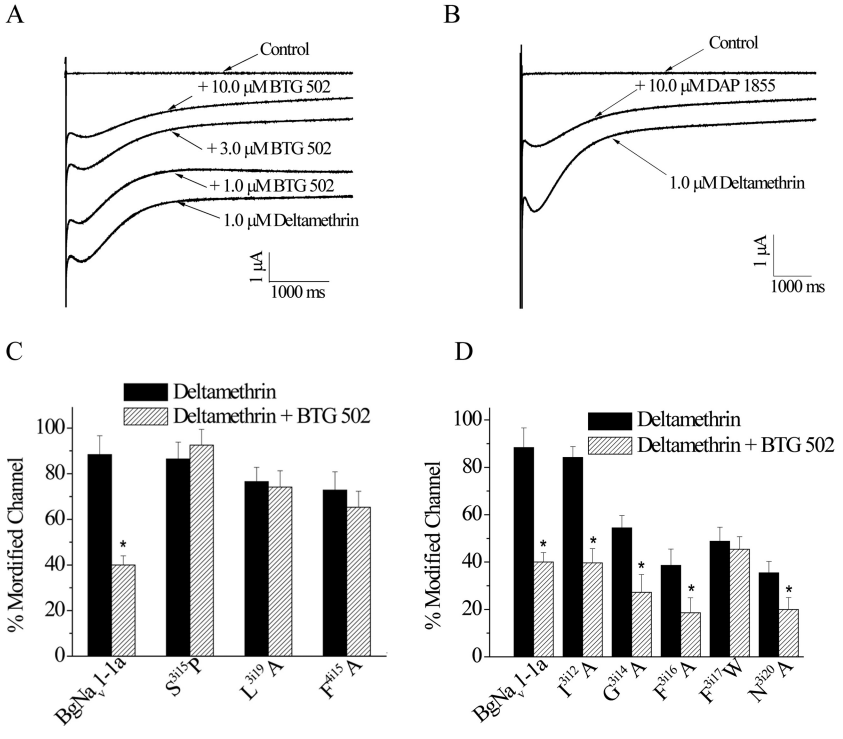

Fig. 3. Effects of BTG 502 and DAP 1855 on the action of deltamethrin on BgNa$_v$1-1a and mutant channels. A and B, inhibition of deltamethrin-induced tail currents by BTG 502 (A) and DAP 1855 (B). C, substitutions at the pore-facing positions S^{3i15}P, L^{3i19}A, and F^{4i15}A abolished BTG 502 antagonism of deltamethrin activity. D, antagonism of BTG 502 on the action of deltamethrin is abolished by mutation F^{3i17}W, but not by alanine substitutions of Ile^{3i12}, Gly^{3i14}, Phe^{3i16}, and Asn^{3i20}. Percentage of channel modification by deltamethrin before (solid bar) and after (stripe bar) the application of 10 μM BTG 502 were calculated using the equation $M = \{[I_{tail}/(E_h - E_{Na})]/[I_{Na}/(E_t - E_{Na})]\} \times 100$. The deltamethrin-induced tail current was recorded after a 100-pulse train of 5-ms step depolarizations from −120 to 0 mV with 5-ms interpulse intervals and a 20-ms test pulse to 0 mV. For the F^{3i16}A, F^{3i17}W, and N^{3i20}A channels, which were 10- to 20-fold more resistant to deltamethrin than the BgNa$_v$1-1a channel (Tan et al., 2005; Du et al., 2009), 10 μM deltamethrin was used. For the I^{3i12}A channel, which was 10-fold more sensitive to deltamethrin than the wild-type (Du et al., 2009), 0.1 μM was used. For the rest of the mutant channels, 1.0 μM was used. The asterisks indicate significant differences after BTG 502 antagonize the action of deltamethrin ($p < 0.05$).

(Fig. 5, A and B). These results suggest that the channel would not close until the toxin left the binding site. Unconstrained MC minimization of the above complex displaced BTG 502 from the horizontal, IIIS6-wrapping mode to a binding mode in which the toxin extended along the pore (Fig. 5, C and D). These calculations suggest that BTG 502 would not bind in the closed channel in the same way it does in the open channel.

Discussion

BTG 502, an *N*-alkylamide insecticide, reduces peak sodium currents of the $BgNa_v$ channel and antagonizes the action of BTX (Du et al., 2011b) and deltamethrin, two sodium channel agonists. Using mutational analysis, we found in this study that seven residues in the $BgNa_v$ channel are essential for the action of BTG 502. These are three key BTX-sensing residues, Ser^{3i15} and Leu^{3i19} in IIIS6 and Phe^{4i15} in IVS6; two deltamethrin-sensing residues, Ile^{3i12} and Phe^{3i17} in IIIS6; and two BTX/deltamethrin-sensing residues, Gly^{3i14} and Phe^{3i16} in IIIS6. We used these data to create an atomistic model of BTG 502 binding to the $BgNa_v$ channel. In this model, BTG 502 wraps around the transmembrane segment IIIS6 and exposes its flexible linker between the bulky ends into the channel pore. This model also shows the interaction of BTG 502 with the pore-facing BTX-sensing residues Ser^{3i15}, Leu^{3i19} and Phe^{4i15}, the deltamethrin-sensing residue Ile^{3i12}, the BTX/deltamethrin-sensing residue Phe^{3i16} in the II/III interface, and the pyrethroid-sensing residue Phe^{3i17} in the III/IV interface. Thus, our results delineate a unique receptor site for BTG 502 on the sodium channel and show that the BTG 502 receptor site overlaps with two receptor sites of BTX and deltamethrin.

BTX, veratridine, aconitine, and grayanotoxin are classified as site 2 toxins. These toxins share common characteristics in their actions on sodium channels: they bind to the sodium channel in its open state, and toxin-modified channels lack fast inactivation and activate at more negative

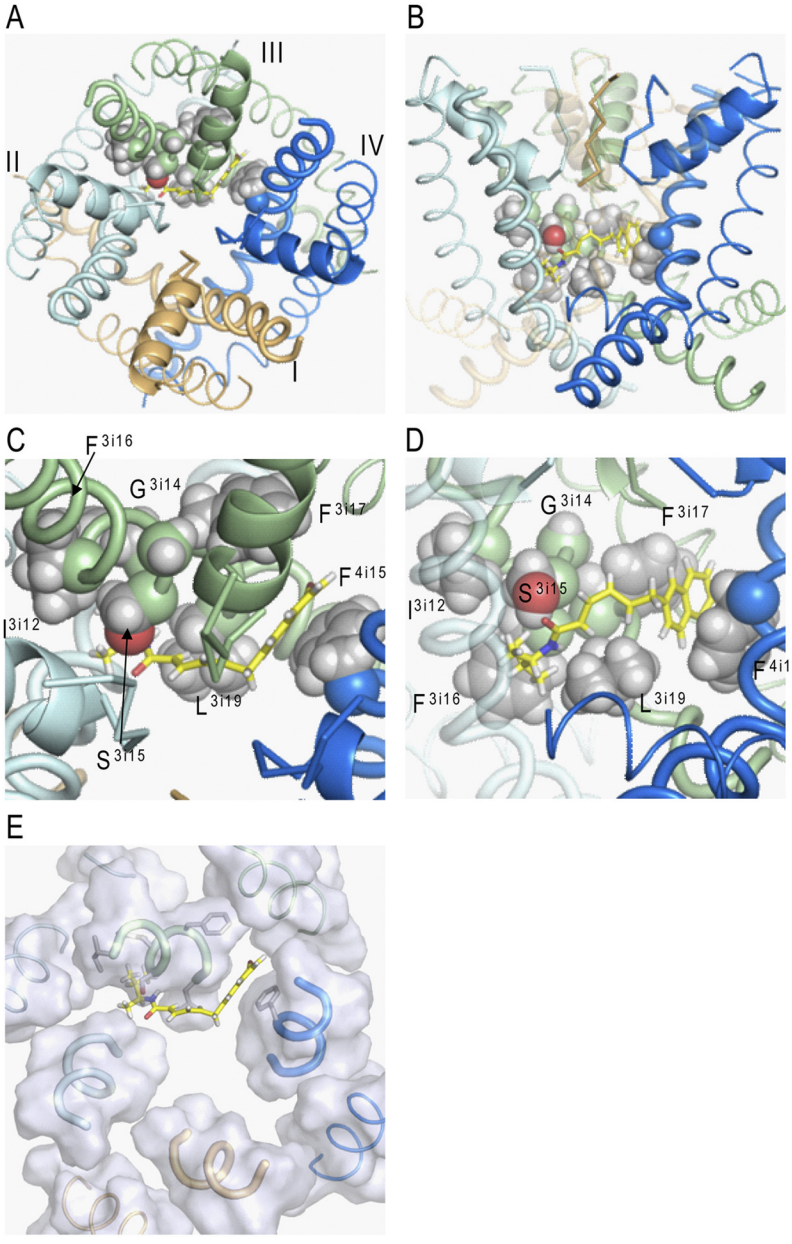

Fig. 4. BTG 502 in the pore domain of BgNav1-1. Repeats I, II, III, and IV are colored brown, gray, green, and blue, respectively. S5s, P-helices, and S6s are shown as thin, medium-sized, and thick helices, respectively. The ascending limbs are shown as thin C-α tracings. The ligand (rendered by sticks with yellow carbons) wraps around IIIS6 and exposes its termini into the II/III and III/IV domain interfaces. Shown are the top (A) and side (B) views and their zoomed images (C and D). E, top view of the pore domain in which parts of the transmembrane helices at the level of the bound BTG 502 are shown by transparent surfaces. In the proposed binding mode, BTG 502 would partially obstruct the ion permeation by the hydrophobic linker exposed into the pore (A, C, and E). The isopropyl group of BTG 502 contacts residues Ile^{3i12} and Phe^{3i16}, which do not face the pore, whereas the amide oxygen accepts an H-bond from Ser^{3i15} (C). Leu^{3i19} is below the hydrophobic linker (D). The naphthalene ring of BTG 502 protrudes in the interface between domains III and IV, where it is flanked by Phe^{3i17} and Phe^{4i15} and forms π-stacking interactions with these residues (C and D).

potentials, resulting in persistent channel activation (Wang and Wang, 2003). Studies of the action of BTG 502 on sodium channels in mouse brain synaptoneurosomes using [^{3}H]batrachotoxinin A-20-α-benzoate binding and $^{22}Na^{+}$ influx assays (Ottea et al., 1989, 1990) and toxin competition experiments in oocyte-expressed insect sodium channels (Du et al., 2011b) show that BTG 502 antagonizes the action of BTX, suggesting that BTG 502 acts at site 2. However, instead of enhancing channel activation as site 2 neurotoxins do, BTG 502 reduces the amplitude of sodium currents, behaving as an antagonist (Du et al., 2011b). The discovery of BTG 502-sensing residues that are either identical to or distinct from BTX-sensing residues and our model of BTG 502 binding in this study can now explain both common and distinct aspects of the binding and action of BTX and BTG 502. Like BTX, BTG 502 binds to open channels, probably entering from the cytoplasmic side. The agonistic effect of BTG 502 when applied to sodium channels in combination with scorpion toxin (Ottea et al., 1989) suggests that BTG 502 stabilizes the open conformation of sodium channels. Whereas BTX induces persistent activation by providing a hydrophilic path for the permeating ions (Du et al., 2011a), the hydrophobic linker between the naphthalene and alkylamide ends of BTG 502 protrudes in the pore lumen (Fig. 4), thus obscuring the ion conducting path and reducing the amplitude of peak sodium current (Fig. 2D). It is noteworthy that BTG 502 increased the amplitude of peak current of several mutant channels (Fig. 2, E and F). These results suggest that BTG 502 can bind to the F^{3i17}A and L^{3i19}A mutant channels without obstructing the pore lumen. These mutations could alter the orientation of BTG 502, thus converting it from an antagonist to a weak activator. Further mutational analysis and molecular modeling of BTG 502 with the mutants will be needed to investigate the molecular basis of this agonistic effect.

According to our model, the putative gating-hinge residue Gly^{3i14} in the middle of IIIS6 is not located within any of the predicted receptor sites for pyrethroids, BTG 502, or BTX. However, it is intriguing that Gly^{3i14} is critical for actions of three sodium channel toxins, BTG 502 (this study), deltamethrin (Du et al., 2009), and BTX (Du et al., 2011a). We have shown previously that the G^{3i14}A substitution causes a positive shift in the voltage dependence of activation (Du et al., 2009), indicating an increased stability of the closed state in the mutant channel and that greater depolarization is needed to activate the channel. We speculate that this gating alteration could provide a basis for the observed involvement of Gly^{3i14} in the actions of BTX, deltamethrin, and BTG 502, because all three toxins require open channels for action. The mutation G^{3i14}A could alter the positions of other toxin-sensing residues, forming a high-affinity receptor site. Alternatively, the mutation of the gating hinge may affect the coupling of toxin binding and subsequent gating modifications induced by the toxin.

Our model also provides an explanation for the antagonism of deltamethrin action by BTG 502 and suggests direct competition between the two toxins for their overlapping receptor sites. It seems that occupation of the receptor site of BTG 502 is sufficient for the antagonism of the activity of deltamethrin, because DAP 1855, an inactive analog of BTG 502, also antagonized the action of deltamethrin (Fig. 3B). Consistent with this notion, residues Ser^{3i15}, Leu^{3i19}, and Phe^{4i15}, which face the pore and contribute to BTX and BTG 502 binding, are all required for BTG 502 to antagonize the deltamethrin action

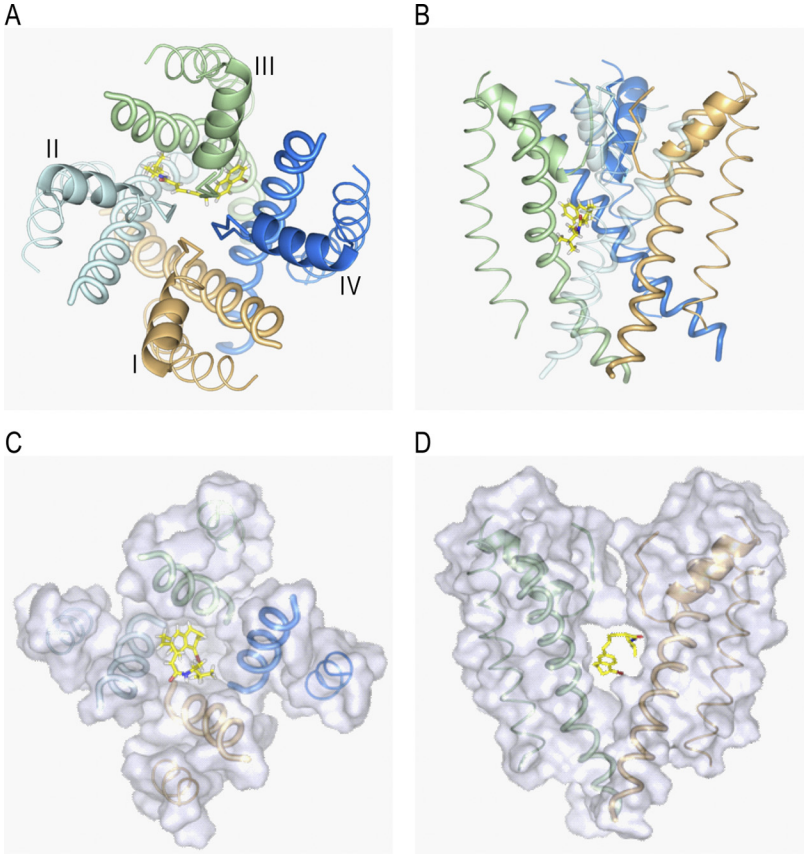

Fig. 5. The closed-channel KcsA-based models of BgNa$_v$1-1 MC minimized with BTG 502. A and B, extracellular and side view of the complex obtained with ligand-channel constraints applied to keep BTG 502 in the binding mode, which has been predicted for the open channel (Fig. 4). To accommodate the toxin, the inner-helix IIIS6 (green) has bent significantly compared with IS6 (orange). Strong toxin-channel repulsions found in the MC-minimized structure (data not shown) indicate that BTG 502 in this binding mode would resist the channel deactivation. C and D, top and side views at the complex obtained without the channel-toxin constraints. BTG 502 relocated from the starting position (A and B) to the central cavity and adopted a folded conformation.

(red symbols in Supplemental Table S2 and red carbons in Supplemental Fig. S2), whereas the pyrethroid-sensing residue Asn^{3i20}, which is not required for BTG 502 inhibition, did not alter BTG 502 antagonism of deltamethrin action. Intriguingly, however, of the four other pyrethroid-sensing residues that are critical for BTG 502 inhibition, only Phe^{3i17} (purple symbols in Supplemental Table S2 and purple carbons in Supplemental Fig. S2), but not Ile^{3i12}, Gly^{3i14}, or Phe^{3i16} (light blue and green symbols in Supplemental Table S2 and respectively colored carbons in Supplemental Fig. S2), is essential for antagonism of deltamethrin action by BTG 502. Our model suggests the following explanation. Ile^{3i12} and Phe^{3i16} are in the II/III interface and interact with the isopropyl end of BTG 502 that is extended into the interface. Mutations at these positions would decrease the interactions and the isopropyl end would turn toward the pore axis. Because in the pyrethroid-bound channel, the II/III interface is occupied by the pyrethroid (O'Reilly et al., 2006), the isopropyl group of BTG 502 cannot bind there. The group would turn away from the II/III interface toward the pore. As a result, the antagonistic action of BTG 502 in the deltamethrin-bound channel would be insensitive to the mutations of Ile^{3i12} and Phe^{3i16}. As far as Gly^{3i14} is concerned, the alanine mutation of this gating hinge would decrease the open state probability and thus binding of BTG 502 in the open channel. This effect of mutation would be opposed by deltamethrin, a channel activator, explaining why the BTG 502 antagonism is not sensitive to the $G^{3i14}A$ mutation.

In summary, using a combination of mutational analyses and computer modeling, our study provides insights into the molecular action of BTG 502 (a unique partial antagonist) on the sodium channel and its antagonism on the actions of two well known classes of sodium channel toxins (i.e., BTX and pyrethroids). Our results emphasize the importance of the pore-forming S6 of domain III and its gating hinge in the binding and actions of three distinct classes of sodium channel neurotoxins.

Acknowledgments

We thank Drs. Kris Silver and Eugenio Oliveira for critical review of the manuscript and Yoshio Nomura and Jung-Eun Lee for making the mutant constructs used in this study.

Authorship Contributions

Participated in research design: Du, Garden, Khambay, Zhorov, and Dong.

Conducted experiments: Du and Garden.

Performed data analysis: Du and Garden.

Wrote or contributed to the writing of the manuscript: Du, Garden, Zhorov, and Dong.

References

Bloomquist JR (1996) Ion channels as targets for insecticides. *Annu Rev Entomol* **41:**163–190.

Bruhova I, Tikhonov DB, and Zhorov BS (2008) Access and binding of local anesthetics in the closed sodium channel. *Mol Pharmacol* **74:**1033–1045.

Canutescu AA, Shelenkov AA, and Dunbrack RL Jr (2003) A graph-theory algorithm for rapid protein side-chain prediction. *Protein Sci* **12:**2001–2014.

Daly JW, Witkop B, Bommer P, and Biemann K (1965) Batrachotoxin. The active principle of the Colombian arrow poison frog, *Phyllobates bicolor*. *J Am Chem Soc* **87:**124–126.

Davies TG, Field LM, Usherwood PN, and Williamson MS (2007) DDT, pyrethrins, pyrethroids and insect sodium channels. *IUBMB Life* **59:**151–162.

Dewar MJ, Zoebisch EG, Healy EF, and Stewart JJ (1985) Development and use of quantum mechanical molecular models. 76. AM1: a new general purpose quantum mechanical molecular model. *J Am Chem Soc* **107:**3902–3909.

Dong K (2007) Insect sodium channels and insecticide resistance. *Invert Neurosci* **7:**17–30.

Du Y, Garden DP, Wang L, Zhorov BS, and Dong K (2011a) Identification of new batrachotoxin-sensing residues in segment IIIS6 of sodium channel. *J Biol Chem* **286:**13151–13160.

Du Y, Khambay B, and Dong K (2011b) An important role of a pyrethroid-sensing residue F1519 in the action of an alkylamide insecticide BTG 502 on the cockroach sodium channel. *Insect Biochem Mol Biol* **41:**446–450.

Du Y, Lee JE, Nomura Y, Zhang T, Zhorov BS, and Dong K (2009) Identification of a cluster of residues in transmembrane segment 6 of domain III of the cockroach sodium channel essential for the action of pyrethroid insecticides. *Biochem J* **419:**377–385.

Elliott M (1977) Synthetic pyrethroids, in *Synthetic Pyrethroids* (Elliott M ed) pp 1–28, ACS Symposium Series No. 42, Washington, DC.

Feng G, Deák P, Chopra M, and Hall LM (1995) Cloning and functional analysis of TipE, a novel membrane protein that enhances *Drosophila para* sodium channel function. *Cell* **82:**1001–1011.

Garden DP and Zhorov BS (2010) Docking flexible ligands in proteins with a solvent exposure- and distance-dependent dielectric function. *J Comput Aided Mol Des* **24:**91–105.

Li Z and Scheraga HA (1987) Monte Carlo-minimization approach to the multiple-minima problem in protein folding. *Proc Natl Acad Sci USA* **84:**6611–6615.

Linford NJ, Cantrell AR, Qu Y, Scheuer T, and Catterall WA (1998) Interaction of batrachotoxin with the local anesthetic receptor site in transmembrane segment IVS6 of the voltage-gated sodium channel. *Proc Natl Acad Sci USA* **95:**13947–13952.

Long SB, Tao X, Campbell EB, and MacKinnon R (2007) Atomic structure of a voltage-dependent K+ channel in a lipid membrane-like environment. *Nature* **450:**376–382.

Narahashi T (2000) Neuroreceptors and ion channels as the basis for drug action: past, present, and future. *J Pharmacol Exp Ther* **294:**1–26.

O'Reilly AO, Khambay BP, Williamson MS, Field LM, Wallace BA, and Davies TG (2006) Modelling insecticide-binding sites in the voltage-gated sodium channel. *Biochem J* **396:**255–263.

Ottea JA, Payne GT, Bloomquist JR, and Soderlund DM (1989) Activation of sodium channels and inhibition of [^{3}H]batrachotoxinin A-20-alpha-benzoate binding by an *N*-alkylamide neurotoxin. *Mol Pharmacol* **36:**280–284.

Ottea JA, Payne GT, and Soderlund DM (1990) Action of insecticidal *N*-alkylamides at site 2 of the voltage-sensitive sodium channel. *J Agric Food Chem* **38:**1724–1728.

Silver KS, Nomura Y, Salgado VL, and Dong K (2009) Role of the sixth transmembrane segment of domain IV of the cockroach sodium channel in the action of sodium channel blocker insecticides. *Neurotoxicology* **30:**613–621.

Soderlund DM (2005) *Sodium Channels: Comprehensive Molecular Insect Science*. Elsevier, New York.

Tan J, Liu Z, Nomura Y, Goldin AL, and Dong K (2002) Alternative splicing of an insect sodium channel gene generates pharmacologically distinct sodium channels. *J Neurosci* **22:**5300–5309.

Tan J, Liu Z, Wang R, Huang ZY, Chen AC, Gurevitz M, and Dong K (2005) Identification of amino acid residues in the insect sodium channel critical for pyrethroid binding. *Mol Pharmacol* **67:**513–522.

Tatebayashi H and Narahashi T (1994) Differential mechanism of action of the pyrethroid tetramethrin on tetrodotoxin-sensitive and tetrodotoxin-resistant sodium channels. *J Pharmacol Exp Ther* **270:**595–603.

Tikhonov DB and Zhorov BS (2005a) Modeling P-loops domain of sodium channel: homology with potassium channels and interaction with ligands. *Biophys J* **88:**184–197.

Tikhonov DB and Zhorov BS (2005b) Sodium channel activators: model of binding inside the pore and a possible mechanism of action. *FEBS Lett* **579:**4207–4212.

Vijverberg HP and van den Bercken J (1990) Neurotoxicological effects and the mode of action of pyrethroid insecticides. *Crit Rev Toxicol* **21:**105–126.

Wang SY, Mitchell J, Tikhonov DB, Zhorov BS, and Wang GK (2006) How batrachotoxin modifies the sodium channel permeation pathway: computer modeling and site-directed mutagenesis. *Mol Pharmacol* **69:**788–795.

Wang SY, Tikhonov DB, Mitchell J, Zhorov BS, and Wang GK (2007a) Irreversible block of cardiac mutant Na+ channels by batrachotoxin. *Channels (Austin)* **1:**179–188.

Wang SY, Tikhonov DB, Zhorov BS, Mitchell J, and Wang GK (2007b) Serine-401 as a batrachotoxin- and local anesthetic-sensing residue in the human cardiac Na^+ channel. *Pflugers Arch* **454:**277–287.

Wang SY and Wang GK (2003) Voltage-gated sodium channels as primary targets of diverse lipid-soluble neurotoxins. *Cell Signal* **15:**151–159.

Warmke JW, Reenan RA, Wang P, Qian S, Arena JP, Wang J, Wunderler D, Liu K, Kaczorowski GJ, Van der Ploeg LH, et al. (1997) Functional expression of *Drosophila* para sodium channels. Modulation by the membrane protein TipE and toxin pharmacology. *J Gen Physiol* **110:**119–133.

Weiner SJ, Kollman PA, Case DA, Singh UC, Chio C, Alagona G, Profeta S, and Weiner PK (1984) A new force field for molecular mechanical simulation of nucleic acids and proteins. *J Am Chem Soc* **106:**765–784.

Weiner SJ, Kollman PA, Nguyen DT, and Case DA (1986) An all atom force-field for simulations of proteins and nucleic-acids. *J Comput Chem* **7:**230–252.

Zhorov BS (1981) Vector method for calculating derivatives of energy of atom-atom interactions of complex molecules according to generalized coordinates. *J Struct Chem* **22:**4–8.

Zhorov BS (1983) Vector method for calculating derivatives of the energy deformation of valence angles and torsion energy of complex molecules according to generalized coordinates. *J Struct Chem* **23:**649–655.

Zhorov BS and Tikhonov DB (2004) Potassium, sodium, calcium and glutamate-gated channels: pore architecture and ligand action. *J Neurochem* **88:**782–799.

Address correspondence to: Ke Dong, Department of Entomology and Genetics and Neuroscience Programs, Michigan State University, East Lansing, MI 48824. E-mail: dongk@msu.edu